Article

Journal of the Brazilian Chemical Society

https://dx.doi.org/10.21577/0103-5053.20240130

J. Braz. Chem. Soc. **2025**, *36*, 2, e-20240130, 1-8

Poly(acrylic acid) and Poly(acrylic acid-*b*-acrylamide) via RAFT: Effect of Composition on Ni^{2+} Binding Capacity

***Rafael T. de Castro*[a] *and Fabio H. Florenzano*[*,a]**

[a]*Departamento de Materiais, Escola de Engenharia de Lorena, Universidade de São Paulo, Estrada Chiquito de Aquino, 1000, Santa Lucrécia, 12612-550 Lorena-SP, Brazil*

Two poly(acrylic acid-*b*-acrylamide) copolymers, and a poly(acrylic acid) homopolymer were synthesized via reversible addition-fragmentation chain transfer (RAFT) polymerization and tested for nickel removal from aqueous media. RAFT was used for better interchain composition homogeneity and to facilitate the synthesis of the block copolymers. Liquid-phase polymer-based retention (LPR) was used to compare the nickel binding capacity. Uptake tests were carried out at pH 3.0, 4.0, and 5.0. Nickel adsorption isotherms in the range of 1 to 7 mmol L^{-1} were achieved and the Langmuir adsorption model was applied. Maximum binding capacity (Q_m) of Ni^{2+} at 298 K depended on the composition of the copolymers and pH. The polyacid block (PAA) was the major structural feature responsible for high values of nickel binding. All materials presented better uptake at higher pH, probably due to polyacid deprotonation and the increase in the electrostatic interactions. Up to approximately 100 mg of nickel *per* gram of homopolymer could be retained at pH = 5.0. Even though the presence of a poly(acrylamide) block decreases the binding capacity compared to PAA, that block has a specific contribution to nickel binding and can also provide better features to the material as better solubilization, and others.

Keywords: hydrophilic block copolymers, RAFT polymerization, nickel removal, liquid-phase polymer-based retention, decontamination

Introduction

Water and soil contamination by toxic metals is a worldwide concern due to their impact on health of human and other organisms and their persistence in the environment.[1-4] On the other hand, metals such as chromium, cadmium, copper, and nickel are essential in many industrial activities with no more benign alternatives so far. Therefore, the treatment of effluents from industries that use those metals is quite relevant to mitigate the effects of their discharge in water bodies or soil, making these activities safer.

Particularly, nickel is useful in many metallurgical processes such as galvanoplasty, and alloy production. However, nickel is toxic. Epidemiological studies show, for instance, a high cancer incidence in animal models and among workers exposed to this element.[5-8] Ionic nickel binds to deoxyribonucleic acid (DNA) *in vitro*, although weakly, and studies have shown its potential to cause damage to that nucleic acid.[5,8]

Polymers are versatile options to build systems for water purification in the most diverse combinations and setups.[9-11] In particular, synthetic functional water-soluble polymers have been studied as options for ionic nickel removal from aqueous media.[12-16] Poly(acrylic acid) (PAA), polyacrylamide (PAm), and others are useful in several removal processes, including in hybrid systems with semipermeable membranes (such as liquid-phase polymer-based retention technique, LPR).[17-19]

One way to achieve affordable polymeric materials for cation binding is to use repeating units found as simple as those in poly(acrylic acid) and polyacrylamide.[20,21] They are inexpensive and easy to obtain. Utilizing different combinations of meres and architectures of the chains are interesting strategies to maximize the performance, with no need to synthesize very complex monomers. Performance in this case is related not only to binding but also to other important properties of the materials such as solubility, viscosity of the solutions, and others.

Contemporary radical polymerization methods as reversible addition-fragmentation chain transfer polymerization (RAFT) have presented new possibilities for designing and obtaining new copolymers from very

*e-mail: fhfloren@usp.br
Editor handled this article: Fernando C. Giacomelli (Associate)

common monomers.[22-24] Even though random copolymers of PAA and PAm obtained by traditional radical copolymerization have been used for cation removal,[21] techniques such as RAFT are mandatory to study composition and architecture effects since they guarantee interchain homogeneity. In contrast, conventional radical copolymerization leads to a mixture of chains with different compositions. Interchain homogeneity is necessary for the isolation of the parameters that are significant for the structure/properties relationship.[23] In other words, the use of RAFT allows all chains to present very similar composition so that the material behavior can be taken as the behavior of all chains and not of a particular set of them. Due also to the large number of monomers that can be polymerized and the possibility of surface-initiated polymerization, RAFT has been applied lately to generate different types of systems for water decontamination.[25,26]

One way to use hydrophilic copolymers in cation removal systems is to enclose their aqueous solutions in a compartment separate from a solution containing the cation by a semi-permeable membrane. That allows the transfer only of small molecules from the external solution to the internal solution (where the polymer is, solubilized and trapped) and *vice-versa*. Once inside, metallic ions are retained specifically by the polymer functional groups, promoting a net transfer of the cation from the external solution to the internal one. This type of approach has been called liquid-phase polymer-based retention (LPR)[19,21,27] and provides a better exposure of the binding sites on the polymers compared to non-soluble ion-exchange resins and other systems. Also, this approach does not disperse any material (polymeric or other) into the environment. After use the LPR device can be removed from the site carrying the original polymeric material, which is chemically stable, and the metal ions captured.

This work evaluated the capacity of different water-soluble homo and block copolymers based on PAA and PAm to bind Ni^{2+} via LPR. All materials were obtained via reversible addition-fragmentation chain transfer polymerization (RAFT) to reach interchain composition homogeneity and to allow the generation of block copolymers. The combination of RAFT and LPR is a new way not only to improve decontamination systems but also to study the structural features that are the most relevant to the efficiency of such systems. The effects of composition and pH on the binding capacity are explored to reach a better understanding of the influence of all those variables on the material binding performance, a necessary step for the design of new and better polymers suitable for Ni^{2+} removal from water effluents and other aqueous media.

Experimental

Materials

Acrylic acid (AA), containing 200 ppm hydroquinone monomethyl ether (MEHQ) as an inhibitor, 99%, acrylamide (Am) suitable for electrophoresis (≥ 99%) and 2-cyano-2-propyl dodecyl trithiocarbonate (high-performance liquid chromatography (HPLC) ≥ 97%, used as CTA), dimethyl sulfoxide (DMSO) and azobisisobutyronitrile (AIBN) were from Sigma-Aldrich (Saint Louis, USA). AIBN was recrystallized from ethanol before use, all the others were used without further purification. A cellulose membrane for dialysis (cutoff: 14 kDa, also from Sigma-Aldrich) was used for the nickel uptake systems (LPR). All other reagents and solvents were PA grade.

Synthesis of PAA macro-CTA

In a flask equipped with a condenser and a thermometer, immersed in a glycerin bath and under an argon atmosphere, acrylic acid, CTA, and DMSO were added. The mixture was previously stirred, and the system purged with argon. AIBN was then added to initiate the reaction. The CTA:initiator molar ratio was 5:1 at the beginning of the reaction. Aliquots were taken during the synthesis for gel permeation chromatography (GPC) analysis. After 4 h of synthesis (70 ºC), the reaction was stopped by letting oxygen in, and the material was washed several times with acetone to remove residual monomer. The product was redissolved in DMSO, precipitated in ethyl acetate, and dried in the oven at 50 ºC[28] after being washed several times with acetone. This polymer will be called macro-CTA hereafter.

Conversion for all aliquots was determined using the monomer and DMSO signals on GPC. The two signals appeared separate in the chromatogram and were confirmed using injections of each pure substance. DMSO, used to solubilize the samples for injection, was considered an internal standard.

Synthesis of block copolymers of PAA-*b*-PAm

For the polymerization of the second block, the macro-CTA was divided into two parts, each one placed into reactor flasks with different quantities of acrylamide to synthesize two distinct copolymers (same PAA block but PAm blocks of different lengths). The reaction was carried out in water at 70 ºC. The same purging process already described was performed. Ammonium persulfate was added to start the polymerization (macro-CTA: initiator molar ratio 5:1). Starting pH was set to 5.4 to increase acrylamide

reactivity.[29] Aliquots were taken throughout the synthesis. After 2 h, the reaction was stopped and the copolymers were precipitated in acetone and dried in the oven at 50 ºC until mass stabilization. Two dissimilar block copolymers were therefore produced: PAA_{319}-*b*-PAm_{959} and PAA_{319}-*b*-PAm_{577} (indexes determined by GPC), having different lengths of the polyacrylamide block and, consequently, different average molar masses.

Gel permeation chromatography (GPC)

A Proeminence (Shimadzu, Kyoto, Japan) system equipped with differential refractive index (RID-10A) and UV detector (SPD-20A) was used. The mobile phase (flow rate: 0.4 mL min^{-1}) consisted of 5×10^{-2} mol L^{-1} phosphate buffer at pH = 7, 0.05% m/v of sodium nitrite, and 0.2 mol L^{-1} of potassium nitrate. Two Phenomenex (Torrance, USA) columns, PolySep-SEC GFC P5000 and P3000 (dimensions 300 × 7.8 mm), and one Phenomenex pre-column, PolySep-SEC GFC P (dimension 35 × 7.8 mm) were used. Molar masses are relative to PEO standards (ReadyCal, Sigma-Aldrich, USA) ranging from 232 to 1.015×10^6 g mol^{-1}).

The diblock copolymer composition (average number of units *per* chain in each block) was based on the relative molar mass of each block as measured by GPC (second block molar mass = total molar mass – first block molar mass).

Fourier transform infrared spectroscopy (FTIR)

Both block copolymers and the macro-CTA were characterized by Fourier transformed infrared spectroscopy (FTIR) in a Prestige 21 from Shimadzu (Kyoto, Japan). Transmittance spectra were collected from 4500 to 500 cm^{-1} (64 scans). Block copolymers were directly measured by attenuated total reflectance (ATR) and potassium bromide (KBr) pellets were made for the macro-CTA. All spectra have been through baseline correction, CO_2 signal elimination and ATR compensation for wavenumber equalization (only for ATR).

Nickel adsorption studies

Nickel binding capacity was analyzed at three different pHs: 3.0, 4.0, and 5.0. The adsorption apparatus was assembled by dissolving 1 g of each polymer in 80 mL of 50 mmol L^{-1} phosphate buffer. 4.0 mL of this solution were transferred to a dialysis membrane bag that was sealed and submerged in 100 mL of buffered solutions with different concentrations of nickel(II) in 125 mL Erlenmeyer flasks. The systems were kept at 25 °C in an orbital shaker until they reached the adsorption equilibrium. For the adsorption isotherms, nickel concentration ranged between 1 and 7 mmol L^{-1}, and the temperature was 25 °C (298 K). The effect of the dilution was considered by using the same apparatus with only the buffer solution (no copolymer) inside the membrane (blank experiments).

To find out the time necessary for the equilibrium adsorption to be reached, a solution at 1 mmol L^{-1} of Ni^{2+} was used and the binding level was measured at several time intervals between 0 to 12 h.

Nickel concentration was determined by UV-Vis spectrophotometry via complexation with dithizone. An Evolution 201-UV-Vis spectrophotometer from Thermo Scientific (Waltham, USA) was used. Dithizone interacts with Ni^{2+} producing a soluble complex called nickel dithizonate [Ni(p-COOH-$HDz)_2$]. Ni^{2+} concentration was determined using a calibration curve at 680 nm, the wavelength that the complex shows its maximum absorption coefficient.[30,31]

To evaluate the adsorption capacity, the Langmuir isotherm model was applied.[32,33] The linearized form of the Langmuir model equation used here is shown below (equation 1). Such an approach allows a better visual evaluation of the fitting, as can be seen in the Supplementary Information section (Figures S1 to S9).

$$\frac{C_e}{Q_e} = \frac{1.C_e}{Q_m} + \frac{1}{K_L Q_m} \quad (1)$$

where C_e refers to the free concentration of the absorbate at equilibrium and Q_e is the mass of absorbate adsorbed *per* mass of absorbent, also at the equilibrium. The Q_m parameter is related to the maximum adsorption capacity (all binding sites fulfilled) and the Langmuir constant K_L accounts for adsorbent-adsorbate interaction forces.[32,34,35]

Results and Discussion

Synthesis of PAA-CTA and GPC analysis

Figure 1 shows the increase in the average molar mass with conversion for the macro-CTA (PAA) synthesis. The constant increase is a strong evidence of a controlled radical reaction. In the same graphic, the ratio Mw/Mn (molecular dispersity, where Mn is the number average molar mass and Mw is the weight average molar mass;) indicates some loss of the reaction control after around 80% of monomer conversion. As the main goal of this first step was to generate a macro-CTA suitable for further extension of a second block, this partial loss in control has no consequence whatsoever.

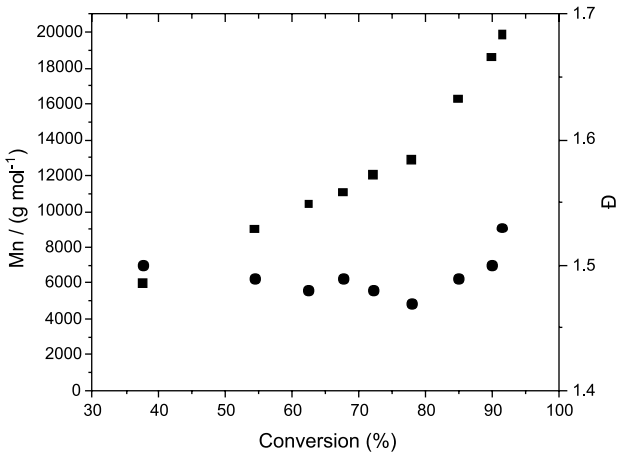

Figure 1. Number average molar mass (■) and molecular dispersity (●) of the PAA macro-CTA during the synthesis via RAFT.

Synthesis of block copolymers of PAA-*b*-PAm and GPC analysis

The molar mass increase of the copolymers (polyacrylamide block polymerization) as a function of the monomer conversion is shown in Figure 2. Both present a linear trend which is strong evidence of polymerization control. The molecular dispersity of the final products (1.28 and 1.29, Table 1) also indicates a controlled polymerization.

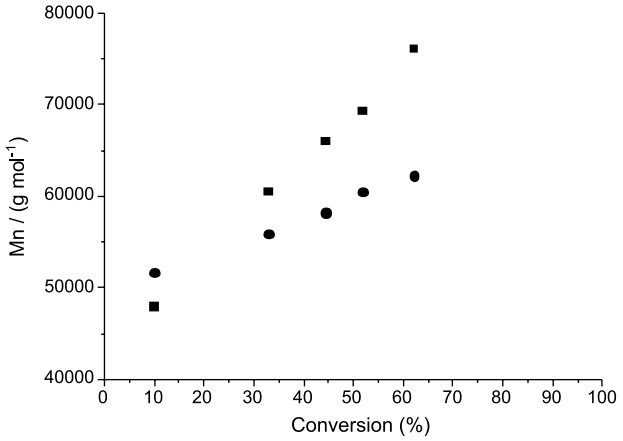

Figure 2. Number average molar mass evolution during the synthesis of PAA_{319}-*b*-PAm_{577} (●) and PAA_{319}-*b*-PAm_{959} (■).

The materials were planned to have different polyacrylamide blocks and the Mn values reached by each one at the highest conversion prove that both reaction behavior as expected, generating two copolymers with different polyacrylamide block sizes. It is worth noting in Figure 2 that Mn is already high (> 40 kg mol^{-1}) at the reaction start, that is because the copolymerization was started with a pre-formed polymer macro-CTA.

Table 1 summarizes the characteristics of all polymeric materials synthesized and used in this work (final purified products).

Table 1. Polymeric materials characterization (GPC) summary

Material	Mn / (kg mol^{-1})	Mw / (kg mol^{-1})	Đ	PAm mass percentage
PAA_{319}-CTA	23.0	35.1	1.52	0
PAA_{319}-*b*-PAm_{577}	64.0	81.9	1.28	47.1
PAA_{319}-*b*-PAm_{959}	91.1	117.4	1.29	59.7

Mn: number average molar mass; Mw: weight average molar mass; Đ: molecular dispersity (Mw/Mn); PAm: polyacrylamide.

FTIR results

The FTIR spectra of all materials are presented in Figure 3. The three materials show a broad signal referring to hydroxyl in the range of 3500-3000 cm^{-1}, associated with the stretching of both the O–H bond (PAA) and the N–H bond (copolymers), and possible moisture absorbed by the materials.[36,37] The signals at 2913 and 2841 cm^{-1} are due to C–H stretching from the main chain of both blocks.[37,38]

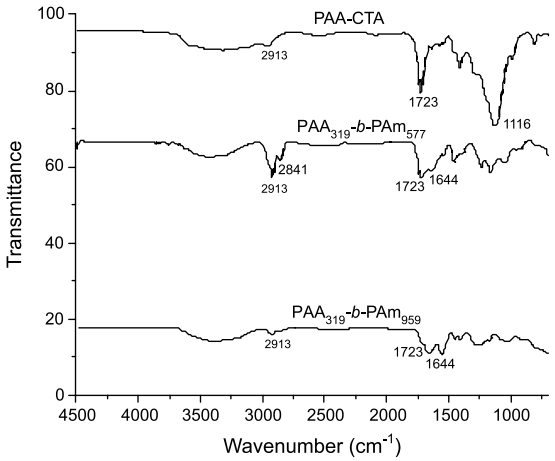

Figure 3. FTIR spectra of the polymeric materials. KBr pellets used for PAA-CTA and ATR for both copolymers.

The signal at 1723 cm^{-1} is due to C=O stretching in carboxylic acids (in this case PAA) and signals in the region of 1650-1640 cm^{-1} are due to the stretching of amide carboxyl (PAm).[36,37,39] This last one is present only in the spectra of copolymers. The C=O amide stretching signal increases relatively if one goes from the copolymer with a smaller polyacrylamide block (PAA_{319}-*b*-PAm_{577}) to that with a larger polyacrylamide block (PAA_{319}-*b*-PAm_{959}), as expected.

The signal in the PAA-CTA spectrum around 1110 cm^{-1} may be related to the stretching of the sulfoxide bond of DMSO used in the macro-CTA purification. This is most likely the case due to the high boiling temperature of DMSO

(189 °C), so the drying process of the macro-CTA may have not been enough to remove all the DMSO from the material.[37,40,41] Such a signal is not present in the spectra of the copolymers, indicating the removal of DMSO during the copolymerization and subsequent purification processes.

Nickel adsorption capacity of polymers

The results of the kinetic binding tests are in Figure 4. The goal was to establish the time necessary for the concentration equilibrium to be reached. All experiments were made with the same initial Ni^{2+} concentration of 1×10^{-3} mol L^{-1}. Equilibrium is reached (Q_e plateau) after approximately 4 h for all materials, so this time was used for the subsequent binding tests with different concentrations (isotherms). For the same pH, the highest Q_e plateau value reached is always for pure polyacid (PAA-CTA). For instance, at pH 5, this plateau is around 30 mg *per* gram of polymer for PAA, and for both PAA-*b*-PAm is within 5 to 15 mg *per* gram, approximately. So, the number of Ni^{2+} binding sites is probably larger in the PAA block than the number of those on the PAm block,[32-34] comparatively to the same mass, since K_L (see below) is not statistically different for the three materials. The control (internal solution with no polymer) is always close to the zero axis ($Q_e = 0$), which demonstrates the specific role played by the polymers.

Table 2 summarizes the Langmuir model parameters obtained from the linearization of the binding isotherms (equation 1) for all polymers and pH studied. The Langmuir model allows one to compare the materials concerning the total capacity of binding (measured by Q_m) and the binding affinity (K_L). Due to the magnitude of the systematic errors for K_L, no further analysis and discussion is permitted, all the K_L values were therefore considered statistically equivalent. Discussion will be focused on Q_m.

The Langmuir Model parameters in Table 2 show that as the pH increases, the cation uptake ratio *per* gram of polymer at the equilibrium (Q_e) also increases significantly for all polymers tested. The deprotonation of the carboxyl groups of the polyacrylic acid, present in all the materials, apparently creates more binding sites[20,34,42,43] for the cation on the (co)polymer chains. This is interesting and points out the fact that the carboxylate binds cation not only more strongly due to the electrostatic interaction but also binds more Ni^{2+} *per* unit than the (non-deprotonated) carboxyl group. This is better demonstrated by the maximum binding capacity (Q_m) which increases with the pH for all materials. This effect has been reported for similar materials.[34,35,44]

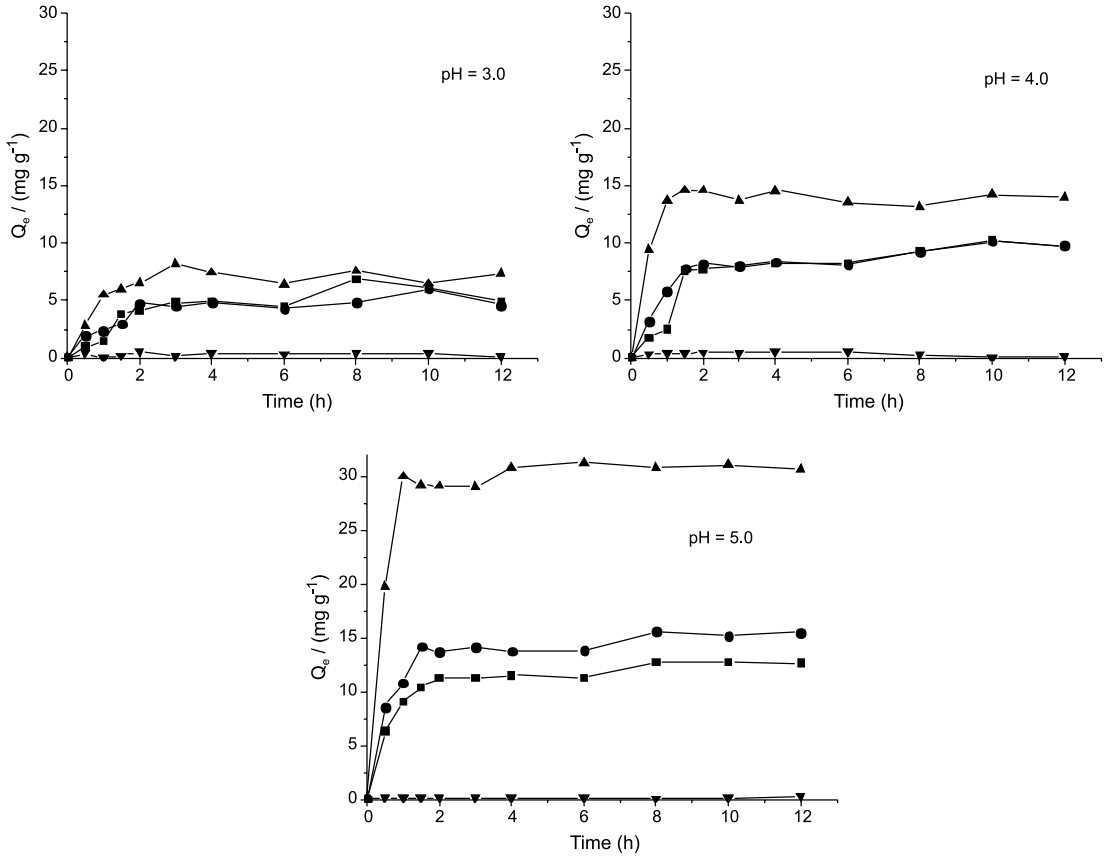

Figure 4. Ni^{2+} adsorption kinetics test. Adsorbent concentration was kept at 1 mmol L^{-1}. (▼) Blank (no polymer), (▲) PAA_{319}-CTA, (●) PAA_{319}-*b*-PAm_{577}, (■) PAA_{319}-*b*-PAm_{959}.

Table 2. Nickel adsorption parameters for each polymer, with adsorbent concentration ranging from 1 to 7 mmol L^{-1} at 298 K (Langmuir model)

Polymer	pH	Langmuir isotherm model parameters		
		Q_m / (mg g^{-1})	K_L / (L mg^{-1})	R
PAA_{319}-CTA	3.0	22.1 ± 3.8	0.006 ± 0.002	0.9368
	4.0	67.9 ± 9.7	0.003 ± 0.001	0.9539
	5.0	99.8 ± 15.5	0.005 ± 0.001	0.9466
PAA_{319}-*b*-PAm_{577}	3.0	10.9 ± 1.6	0.009 ± 0.003	0.9548
	4.0	37.2 ± 6.8	0.004 ± 0.001	0.9297
	5.0	46.5 ± 7.2	0.008 ± 0.003	0.9470
PAA_{319}-*b*-PAm_{959}	3.0	9.6 ± 1.5	0.015 ± 0.016	0.9441
	4.0	23.5 ± 3.3	0.007 ± 0.002	0.9559
	5.0	47.2 ± 7.7	0.008 ± 0.003	0.9420

Q_m: Ni^{2+} mass bound at saturation *per* gram of polymer; K_L: Langmuir constant; R: Pearson's correlation coefficient.

It is important to emphasize that at least 50% of the maximum binding (Q_m) was reached for all isotherms, so, taking also into account that K_L values are all in the same order of magnitude, then Q_m can be considered a good measurement of the materials binding performance within the concentration range studied (1 to 7 mmol L^{-1}) and above.

Concerning composition, at the same pH, Q_m increases with the PAA content, suggesting that the carboxyl functional groups bind more Ni^{2+} than the NH_2 *per* group in the polymer chain. However, the binding due to the PAm block cannot be neglected. Table 3 indicates that the presence of PAm improves the total binding capacity since the copolymers have a Q_m higher than expected for the specific PAA content of each one alone. The PAm contribution to the Ni^{2+} binding varies from approximately 24 to 47% of the total binding capacity of the copolymers. Materials bearing amide groups are known to bind cations due to their lone electron pairs.[15,26,27]

The drop in the specific cation binding capacity as the PAm block molar mass increases occurs at all pHs. The presence of a PAm block might suggest a less strong dependence on binding on pH. That is not the case. The two copolymers show a quite similar increase in the binding capacity compared to the homopolymer with pH. Binding capacity rises around 4 times going from pH = 3.0 to pH = 5.0 for all materials.

Even though the presence of the PAm block causes, therefore, a decrease in the cation binding capacity *per* gram of material, that may be compensated by other properties provided by that block, such as lower specific viscosity, better and faster solubilization, and others, studies still to be performed.

It is also worth mentioning that values up to around 100 mg of Ni^{2+} *per* gram of material were reached (10% of the polymer in mass), indicating the potential of these materials as cation removers. According to Vakili *et al.*,[45] in a 2021 review about Ni^{2+} removal, the most efficient polymer materials so far were able to bind up to around 50 mg *per* gram of polymer, reached by Coskun *et al.*[46]

Table 3. Correlation between the composition of each synthesized polymer and the Q_m parameter obtained by the Langmuir model

Material	pH	Q_m / (mg g^{-1})	Q_m predict due to PAA content only[a] / (mg g^{-1})	Q_m due to PAm / %
PAA_{319}-CTA	3.0	22.1 ± 3.8	22.1	–
	4.0	67.9 ± 8.7	67.9	–
	5.0	99.8 ± 15.5	99.8	–
PAA_{319}-*b*-PAm_{577}	3.0	10.9 ± 1.6	7.9	27.5
	4.0	37.2 ± 6.8	24.2	34.9
	5.0	46.5 ± 7.2	35.5	23.7
PAA_{319}-*b*-PAm_{959}	3.0	9.6 ± 1.5	5.5	42.7
	4.0	23.5 ± 3.3	16.9	28.1
	5.0	47.2 ± 7.7	24.9	47.2

[a]Qm expected if the polyacrylamide block had no binding capacity whatsoever. Q_m: Ni^{2+} mass bound at saturation *per* gram of polymer; PAA: poly(acrylic acid); PAm: polyacrylamide.

Conclusions

Three polymeric materials, one homopolymer (PAA_{319}) and two copolymers bearing both the same PAA block (PAA_{319}-*b*-PAm_{577} and PAA_{319}-*b*-PAm_{959}), have shown good Ni^{2+} binding properties and were studied under different conditions. The materials were obtained by RAFT to guarantee a good interchain composition homogeneity. The specific total removal capacity, measured via Q_m (Langmuir adsorption model), at 298 K, increased with the pH, most likely due to PAA deprotonation. The Q_m ranged from around 9 to 100 mg *per* gram of polymer, depending on the material and the pH. A binding capacity of approximately 10% of metal by mass can be considered a very high value for a synthetic polymer.

PAA_{319} showed the best total binding capacity, *per* gram, out of the three materials at the same pH. The presence of the PAm block reduces Q_m, and the effect of the pH was still present in the same magnitude compared to the PAA homopolymer, an unexpected result. The binding capacity of the copolymers was due to both the PAA and PAm blocks which indicates that it is not only mediated by electrostatic interactions but also by lone pair complexation.

Block copolymers may be preferable in field applications, despite the lower performance presented here compared to the PAA homopolymer, due to properties such as lower specific viscosity, better and faster precipitation, and fewer solubilization issues. All materials are to be tested with different metals in the search for selectivity, as well as, they are to be modified to reach more robust relationships of the binding capacity and the chemical structure.

This work has therefore shown the potential of the three materials studied here as Ni^{2+} removers from aqueous media and identified the contribution of the PAm block to the binding of the cation. Potential applications of the materials and systems described here are foreseen in mining and other activities that generate aqueous effluents contaminated with nickel and other toxic metals.

Supplementary Information

Supplementary data (binding isotherms) are available free of charge at http://jbcs.sbq.org.br as PDF file.

Acknowledgments

This study was financed in part by the Coordenação de Aperfeiçoamento de Pessoal de Nível Superior - Brasil (CAPES) - Finance Code 001, process number: 88882.379232/2019-01. FHF thanks FAPESP research grants 2013/08166-5 and 2022/02049-6 and CNPq 457733/2014-4.

Author Contributions

FHF was in charge of conceptualization, data curation, formal analysis, funding acquisition, project administration, resources, writing review, and editing. RTC was in charge of conceptualization, data curation, formal analysis, investigation, and writing the original draft.

References

1. Van Tran, V.; Park, D.; Lee, Y.-C.; *Environ. Sci. Pollut. Res.* **2018**, *25*, 24569. [Crossref]
2. Rivas, B. L.; Sánchez, J.; Urbano, B. F.; *Polym. Int.* **2016**, *65*, 255. [Crossref]
3. Corti, G. S.; Botaro, V. R.; Gil, L. F.; Gil, R. P. F.; *Polímeros* **2004**, *14*, 313. [Crossref]
4. Tapiero, Y.; Rivas, B. L.; Sánchez, J.; Bryjak, M.; Kabay, N.; *J. Appl. Polym. Sci.* **2015**, *132*, 41953. [Crossref]
5. Das, K. K.; Das, S. N.; Dhundasi, S. A.; *Indian J. Med. Res.* **2008**, *128*, 412. [Link] accessed in July 2024
6. Agency for Toxic Substances and Disease Registry; *Toxicological Profile for Nickel*, https://wwwn.cdc.gov/TSP/ToxProfiles/ToxProfiles.aspx?id=245&tid=44, accessed in July 2024.
7. Cempel, M.; Nikel, G.; *Polish. J. Environ. Stud.* **2006**, *15*, 375. [Link] accessed in July 2024
8. Doreswamy, K.; Shrilatha, B.; Rajeshkumar, T.; Muralidhara; *J. Androl.* **2004**, *25*, 996. [Crossref]
9. Pandey, S.; Son, N.; Kang, M.; *Int. J. Biol. Macromol.* **2022**, *210*, 300. [Crossref]
10. Rivas, B. L.; Urbano, B. F.; Sanchez, J.; *Front. Chem.* **2018**, *6*, 320. [Crossref]
11. Alaba, P. A.; Oladoja, N. A.; Sani, Y. M.; Ayodele, O. B.; Mohammed, I. Y.; Olupinla, S. F.; Daud, W. M. W.; *J. Environ. Chem. Eng.* **2018**, *6*, 1651. [Crossref]
12. Basak, U.; Ghosh, R.; Ghosh, T.; Majumdar, S.; Pakhira, M.; Ghosh, T.; Chatterjee, D. P.; *Polymer* **2018**, *155*, 27. [Crossref]
13. Wong, A.; de Oliveira, F. M.; Tarley, C. R. T.; Sotomayor, M. P. T.; *React. Funct. Polym.* **2016**, *100*, 26. [Crossref]
14. Abdel-Halim, E. S.; Al-Deyab, S. S.; *Carbohydr. Polym.* **2011**, *86*, 1306. [Crossref]
15. dos Santos, P. M.; Corazza, M. Z.; Tarley, C. R. T.; *Food Chem.* **2024**, *440*, 138238. [Crossref]
16. Xu, H.; Liang, Y.; Zhu, F.; *J. Water, Chem. Technol.* **2023**, *45*, 533. [Crossref]
17. Fan, C.; Li, K.; Wang, Y.; Qian, X.; Jia, J.; *RSC Adv.* **2016**, *6*, 2678. [Crossref]
18. Ulbricht, M.; *Polymer* **2006**, *47*, 2217. [Crossref]

19. Rivas, B. L.; Pereira, E. D.; Palencia, M.; Sanchez, J.; *Prog. Polym. Sci.* **2011**, *36*, 294. [Crossref]
20. Li, W.; Zhao, H.; Teasdale, P. R.; John, R.; Zhang, S.; *React. Funct. Polym.* **2002**, *52*, 31. [Crossref]
21. Rivas, B. L.; Moreno-Villoslada, I.; *Macromol. Chem. Phys.* **1998**, *199*, 1153. [Crossref]
22. Florenzano, F. H.; *Polímeros: Ciência e Tecnologia* **2008**, *18*, 100. [Link] accessed in July 2024
23. Moad, G.; *Polym. Chem.* **2016**, *8*, 177. [Crossref]
24. Chiefari, J.; Chong, Y. K.; Ercole, F.; Krstina, J.; Jeffery, J.; Le, T. P. T.; Mayadunne, R. T. A.; Meijs, G. F.; Moad, C. L.; Moad, G.; Rizzardo, E.; Thang, S. H.; *Macromolecules* **1998**, *31*, 5559. [Crossref]
25. Yılmaz, Ş.; Zengin, A.; Şahan, T.; Zorer, Ö. S.; *Environ. Technol. Innovation* **2021**, *23*, 101631. [Crossref]
26. Yılmaz, Ş.; Zengin, A.; Şahan, T.; *Colloids Surf., A* **2021**, *612*, 125979. [Crossref]
27. Sánchez, J.; Bastrzyk, A.; Rivas, B. L.; Bryjak, M.; Kabay, N.; *Polym. Bull.* **2013**, *70*, 2633. [Crossref]
28. Palmiero, U. C.; Chovancova, A.; Cuccato, D.; Storti, G.; Lacik, I.; Moscatelli, D.; *Polymer* **2016**, *98*, 156. [Crossref]
29. Rintoul, I.; Wandrey, C.; *Polymer* **2005**, *46*, 4525. [Crossref]
30. Ntoi, L. L. A.; Buitendach, B. E.; von Eschwege, K. G.; *J. Phys. Chem. A* **2017**, *121*, 9243. [Crossref]
31. von Eschwege, K. G.; Conradie, J.; Kuhn, A.; *J. Phys. Chem. A* **2011**, *115*, 14637. [Crossref]
32. Foo, K. Y.; Hameed, B. H.; *Chem. Eng. J.* **2010**, *156*, 2. [Crossref]
33. Giles, C. H.; MacEwan, T. H.; Nakhwa, S. N.; Smith, D.; *J. Chem. Soc.* **1960**, 3973. [Crossref]
34. Orozco-Guareño, E.; Santiago-Gutiérrez, F.; Morán-Quiroz, J. L.; Hernandez-Olmos, S. L.; Soto, V.; de la Cruz, W.; Manríquez, R.; Gomez-Salazar, S.; *J. Colloid Interface Sci.* **2010**, *349*, 583. [Crossref]
35. Sutirman, Z. A.; Sanagi, M. M.; Abd Karim, K. J.; Wan Ibrahim, W. A.; Jume, B. H.; *Int. J. Biol. Macromol.* **2018**, *116*, 255. [Crossref]
36. Lin, C.-L.; Lee, C.-F.; Chiu, W.-Y.; *J. Colloid Interface Sci.* **2005**, *291*, 411. [Crossref]
37. Pavia, D. L.; Lampman, G. M.; Kriz, G. S.; Vyvyan, J. R.; *Introdução à Espectroscopia*, 4th ed.; Cengage: São Paulo, Brazil, 2010.
38. Yan, H.; Yang, L.; Yang, Z.; Yang, H.; Li, A.; Cheng, R.; *J. Hazard. Mater.* **2012**, *229*, 371. [Crossref]
39. Sanchez, L. M.; Martin, D. A.; Alvarez, V. A.; Gonzalez, J. S.; *Colloids Surf., A* **2018**, *543*, 28. [Crossref]
40. Zhang, W.; Jiang, Y.; Ding, Y.; Zheng, M.; Wu, S.; Lu, X.; Gao, X.; Wang, Q.; Zhou, G.; Liu, J.; Naughton, M. J.; Kempa, K.; Gao, J.; *Opt. Mater. Express* **2017**, *7*, 2150. [Crossref]
41. Lambert, J. B.; *Introduction to Organic Spectroscopy*; Macmillan: New York, USA, 1987.
42. Abd El-Mohdy, H. L.; Hegazy, E. A.; El-Nesr, E. M.; El-Wahab, M. A.; *Arabian J. Chem.* **2016**, *9*, S1627. [Crossref]
43. Nesrinne, S.; Djamel, A.; *Arabian J. Chem.* **2017**, *10*, 539. [Crossref]
44. Reddy, D. H. K.; Lee, S.-M.; *J. Appl. Polym. Sci.* **2013**, *130*, 4542. [Crossref]
45. Vakili, M.; Rafatullah, M.; Yuan, J.; Zwain, H. M.; Mojiri, A.; Gholami, Z.; Gholami, F.; Wang, W.; Giwa, A. S.; Yu, Y.; Cagnetta, G.; Yu, G.; *Rev Chem. Eng.* **2021**, *37*, 755. [Crossref]
46. Coskun, R.; Soykan, C.; Saçak, M.; *Sep. Purif. Technol.* **2006**, *49*, 107. [Crossref]

Submitted: February 16, 2024
Published online: July 22, 2024